Code	CP4OCCN-D33-01	**Edition**	1.2	**Date**	24/02/16
Client	European Space Agency	**Final User**		-	

ESA Support to Science Element (STSE)
CryoSat+: Ocean Theme

CP4O – CryoSat Plus 4 Oceans – CCN1

ESA AO/1-6827/11/I-NB

D3.3.
WP3000 - SAMOSA SAR retracker improvements- Assessment of Evaluation Data Set

	Name	Signature	Date
Written by	SatOC (Marcello Passaro and David Cotton)		24/02/16
Approved by	Ellis Ash		
Revised by			
Authorised by	David Cotton		

DISSEMINATION	COPIES	MEANS
ESA: Jérôme Benveniste, Américo Ambrózio, Marco Restano	1	Electronic
SatOC: David Cotton, Marcello Passaro	1	Electronic
DTU Space: Ole Andersen	1	Electronic
isardSAT: Monica Roca, Pablo Nilo Garcia	1	Electronic
NOC: Paolo Cipollini	1	Electronic
Noveltis: Mathilde Cancet	1	Electronic
STARLAB: Francisco Martin, Antonio Repucci	1	Electronic

SUMMARY OF MODIFICATIONS

Ed.	Date	Chapter	Modification	Author/s
1.0	01/12/15	All	First Draft	SatOC
1.1	08/02/16	various	Updates following ESA review	SatOC
1.2	24/02/16	Various	Further edits and formatting changes	SatOC

TABLE OF CONTENTS

LIST OF FIGURES AND TABLES

ACRONYMS AND ABBREVIATIONS

ATBD	Algorithm Theoretical Basis Document
CCN	Contract Change Notice
CLS	Collecte Localisation Satellites
CNES	Centre National d'Etudes Spatiales
CNES-CPP	CNES CryoSat Processing Prototype
CP4O	CryoSat Plus for Oceans
CryoSat, C2	ESA satellite altimeter Crysophere mission, which operates a SAR mode altimeter
ESA	European Space Agency
ESRIN	ESA Centre for Earth Observation / ESA Space Research Institute
FBR	Full Bit Rate data
GPOD	Grid Processing on Demand (ESA Service at https://gpod.eo.esa.int/)
Jason-2	US/French Satellite Altimeter Mission
LRM	"Low Resolution Mode" - "conventional", pulse limited, altimeter mode / product
MAD	Median Absolute Deviation
NOC	National Oceanography Centre, UK
Pu	Received Power
RADS	Radar Altimeter Database System. Global altimeter database maintained by TU Delft
SAMOSA	Analytical SAR altimeter ocean echo model developed in SAMOSA project.
SAR	Synthetic Aperture Radar
SatOC	Satellite Oceanographic Consultants, UK
Sigma-0, σ^0	Surface radar backscatter at normal incidence
SIRAL	The altimeter (with SAR mode operation) on CryoSat-2
SSH	Sea Surface Height
Std	Standard Deviation
STSE	Support to Science Element
SWH	Significant Wave Height

REFERENCE DOCUMENTS

[RD1] Boy, F. and Moreau, T., 2013: Algorithm Theoretical Basis Document (ATBD) of the CPP SAR numerical retracker for oceans. CNES report reference *S3A-N-SRA-00099-CNES*, Version 1.0, 15/06/2013, 16 pp.
(http://www.satoc.eu/projects/CP4O/docs/S3A-NT-SRAL-00099-CNES_SAR_ATBD.pdf)

[RD2] Dinardo, S., 2014: GPOD CryoSat-2 SARvatore Software Prototype User Manual, Available from: *https://wiki.services.eoportal.org/tiki-index.php?page= GPOD+CryoSat-2+SARvatore+Software+Prototype+User+Manual*

[RD3] Ray, C., Martin-Puig, C., Clarizia, M-P, Ruffini, G., Dinardo, S., Gommenginger, C.P. and Benveniste, J., 2015: SAR Altimeter Backscattered Waveform Model, IEEE Trans. GeoSc. Remote Sensing, Vol 53, Issue 2, pp911-919. DOI 10.1109/TGRS.2014.2330423

[RD4] Gommenginger, C. and Cipollini, P., 2014: CP4O CryoSat Plus 4 Oceans WP4000 Product Development and Validation. ESRIN report reference ESA AO/1-6827/11/I-NB (http://www.satoc.eu/projects/CP4O/docs/CP4O_WP4_SAR_OceanCoastal_PVR_v1.0.pdf)

[RD5] Martin, F. et al., 2015: Improved Estimation of Thermal Noise in the SAMOSA retracker. CP4O CCN01 D3.1 Technical Note

ACKNOWLEDGMENTS

This extension to the CP4O project has been funded by ESA under the Support to Science Element (STSE) programme

We wish to acknowledge the support of CNES and CLS who kindly provided the CNES-CPP data used in this work. CNES-CPP products were developed by CNES and CLS in the frame of the "Sentinel-3 SRAL SAR mode performance assessment" study.

1 INTRODUCTION: OBJECTIVES AND APPROACH

The objective of WP3000 of the CP4O CCN01 is to implement and evaluate a key potential improvement to the SAMOSA SAR altimeter data re-tracker that is currently applied within the Sentinel-3 processing chain (RD2, RD3), thus potentially leading to recommendations for modifications to this implementation.

The aim of this improvement is to provide an optimised estimation of thermal noise, which should then improve the representation of the leading edge in the analytic SAMOSA model and subsequently also improve the estimation of Significant Wave Height. Full details are given in a separate Technical Note prepared by Starlab (RD5).

After developing, testing and implementing the improvements to the SAMOSA re-tracker, Starlab then generated an evaluation data set, to be independently assessed by SatOC. The evaluation was carried out by SatOC, by comparing the parameters in the evaluation data set against other satellite altimeter data: CryoSat CNES-CPP L2 data (RD1), Jason-2 data, and against in-situ (buoy) data. The validation focuses on Sea Surface Height (SSH), Significant Wave Height (SWH), and Receive Power (Pu), linked to the Normalised Radar Cross Section (σ^0). In this report the SSH for Starlab and CNES-CPP is always calculated as a simple Altitude – Range difference, where no geophysical corrections are included.

This report presents the SatOC validation of the Starlab evaluation data set. To support comparison, this work was carried out in a similar way, and presented in a similar format, as the CP4O WP4000 Product Validation Report for SAR Altimetry over the Open Ocean and Coastal Zone (RD4).

2 EXPERIMENTAL DATA SETS

2.1 The Evaluation Data Set

The SAR altimeter Evaluation Data Set was generated by Starlab, using the modified SAMOSA SAR mode re-tracker, for the period 01/11/12 to 31/12/13, and the area 30°-65°N, 20°-0°W, using as input the CNES-CPP (V14) CryoSat L1B data set. The CPP data set was used as a source so that it would be possible to directly compare the performance of the modified SAMOSA (analytical) retracker and the numerical re-tracker implemented in the CPP product, starting from the same source L1B data set. By using the same source L1B data set for both re-trackers we can be certain that any differences in the final product are due only to the re-trackers used. Also we wished to maintain continuity with the previous analyses from the main CP4O contract, which were primarily based on CPP L1B data.

Hereafter the data retracked by the modified SAMOSA re-tracker, the evaluation data set, will be referred to as the Starlab data set. Description of this data set can be found in the Appendix to RD5.

2.2 Validation Data

The Evaluation Data Set was validated against satellite and in-situ data, as follows:

Satellite Altimeter Data

- CryoSat CNES-CPP (V14) L2 data for the same period and location as the Starlab evaluation data set, produced from the same source CNES-CPP L1B data. Hereafter this data set is referred to as CNES-CPP.
- Jason-2 altimeter data were downloaded from the Radar Altimetry Database Service (RADS) for the same period and location as the Starlab evaluation data set.

In Situ Data

The wave buoy data used for validation consists of data from UK Met Office buoys, located > 25km from land. The location of the buoys is shown in Figure 1. Due to limited coverage of the Starlab evaluation data set, the comparison with CNES-CPP excludes buoys 62163 and 62001.

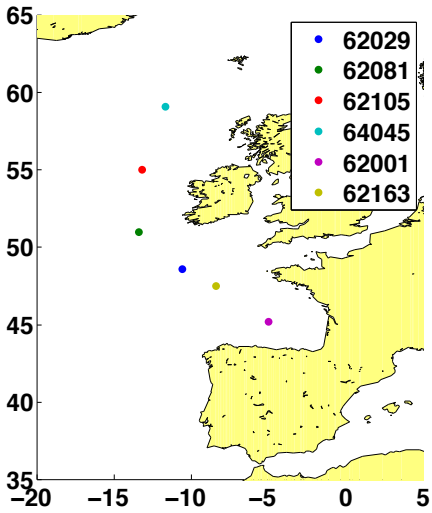

Figure 1: Location of UK Met Office buoys used for validation

3 ALTIMETER DATA DIAGNOSTICS AND PREPARATION

3.1 Misfit

The misfit captures the quality of the fit between the L1B waveform and the fitted model. The misfit is particularly well suited to detect imperfect fitting, for example in the case of low SWH. Hence, together with the value of the misfit, its behaviour against SWH is also of interest. (See also RD.4)

In CNES-CPP, the misfit is calculated as the root mean square of sum of the residuals, scaled by the number of bins in the waveform:

$$misfit\_CPP = 100.* sqrt(1/104.*\Sigma(residual^2))$$

where the residual is the difference between the fitting and the real waveform at each bin, scaled by the maximum of the waveform values, as follows.

$$residual = (model - data\ (13:116))/Max\_data$$

$$Max\_data=max(data(13:116)$$

$$data = waveform\_data$$

$$model = waveform\_model$$

In the Starlab evaluation data set, the residuals are not scaled by this factor, which makes the comparison impossible, as seen in Sections 4.1 and 4.2.1.

It is recommended that for future studies a consistent calculation of misfit is applied.

3.2 Altimeter versus Buoy SWH

Scatter plots of C2 SAR SWH versus buoy SWH are presented, supported by estimates of the mean and standard deviation of the SWH bias, where SWH bias is defined as:

$$SWH\_bias = SWH\_Alt - SWH\_Buoy$$

The dataset is obtained by collocating the altimeter data with the buoy, to within 1 hour and 50km.The same approach can be applied to other altimeter data e.g. Jason-2, thus supporting direct comparison of the performance of C2 SAR SWH with those of conventional LRM altimeters. (This is the same approach as was applied in RD.4)

3.3 Outlier Removal

Unrealistic and land contaminated detections are removed from both datasets. In particular, a 20 Hz estimation is removed when

- $SWH > 15$ m
- $abs(Altitude - Range) > 100\ m$ *(note that no geophysical corrections are included)*
- $SWH = 0\ m$ (0.1 m for CNES-CPP, since it is observed from the data that this is the value that the parameter assumes in case of erroneous estimation (Martin, pers. comm. 2015).

From high-rate waveforms, Starlab and CNES-CPP retracked SWH and SSH are then averaged to generate 1 Hz estimations. A check is performed in order to eliminate further outliers: on every block of 20 high-rate values X, the median value and the median absolute deviation (MAD) are computed. Each estimation x is considered valid if:

$$median\ (X) - 3 \text{ x } MAD(X) < x < median(X) + 3 \text{ x } MAD(X)$$

where

$$MAD(X) = 1.4286 \text{ x } median(|X\text{-}median(X)|)$$

The MAD computed using the factor 1.4286 is considered equal to the standard deviation for a normal distribution. Once the outliers have been excluded, the median of the remaining points is computed in order to generate the 1 Hz estimation.

3.4 Coverage of Re-tracked data

When the dataset from STARLAB was delivered, it was found that the coverage of the re-tracked CryoSat evaluation data set was not complete, as many records were not processed due to “contaminated” waveforms. This affected up to 60% of the data records in the data set (RD5), to the extent that neither valid data close to the UK coast, nor cross-overs within 50km of buoys 62001 or 62163 were available. This significantly restricted the possible analysis in terms of validation against buoy data.

4 RESULTS OVER THE OPEN OCEAN

4.1 Along Track Example

Figure 2 shows an example of parameter estimation (for SWH, uncorrected SSH and Pu) from a C2 data segment recorded on the 3rd of January 2013. The agreement between CNES-CPP and Starlab is visually evident and confirmed by the plot of the differences in Figure 3, again the differenced SSH values are uncorrected (note that the residuals for the different parameters are not scaled to the same factor). Nevertheless, as anticipated in 3.1, the bottom plot of Figure 2 shows that the misfit does not have any correspondence in the two datasets. For this reason, no misfit threshold is applied in this validation. The "STARLAB" parameters represented in Figures 2 and 3 are taken from the Starlab produced evaluation data set (as described in the RD5 appendix), and "CPP" values from the original CPP data set. Note however that because the corrections to the SSH are not applied consistently to the STARLAB and CPP data sets, to allow a direct comparison the "STARLAB" uncorrected SSH in Figures 2 and 3 is calculated as 'altitude CPP - range STARLAB'.

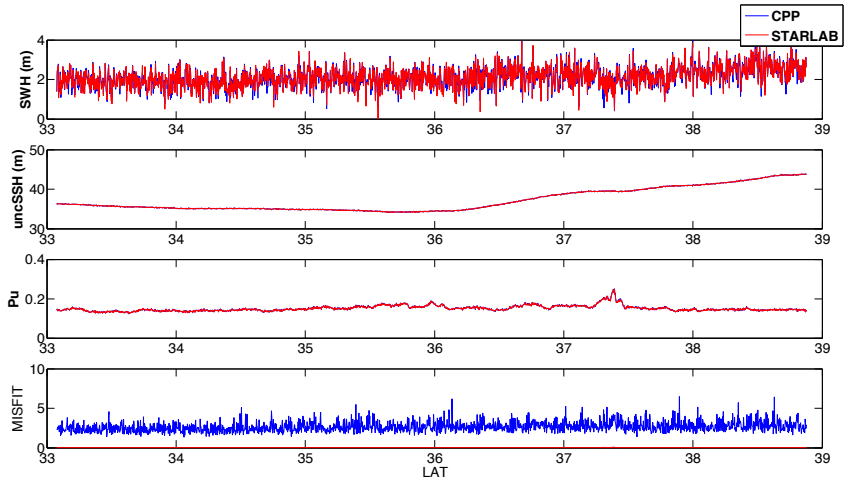

Figure 2: Example of parameter estimation for a segment of C2 SAR track, using CNES-CPP and Starlab. File: CS_OPER_SIR1TKSA0__20130103T053440_20130103T053652

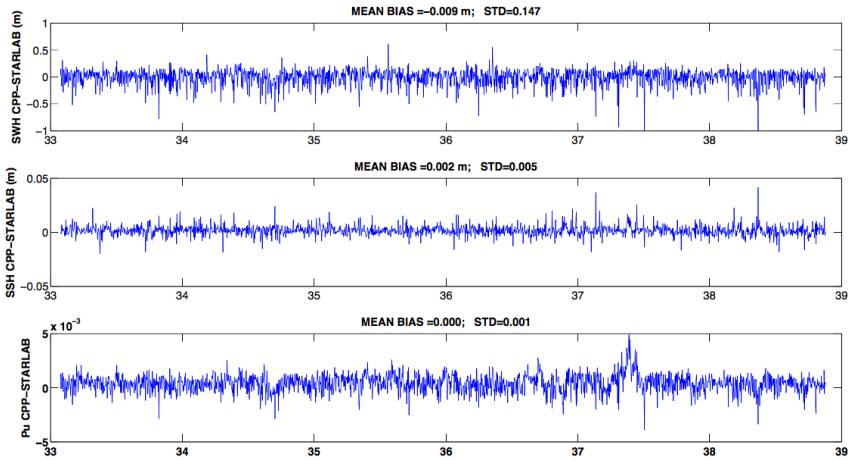

Figure 3: Difference between CNES-CPP and Starlab estimations for file CS_OPER_SIR1TKSA0__20130103T053440_20130103T053652 in the along-track segment.

The mean bias and standard deviation of the differences (std) are reported on top of the plots in Figure 3. The mean bias is below 1 cm for both SWH and SSH. Some spikes where Starlab overestimates the SWH and underestimate the SSH compared to CNES-CPP are present.

4.2 Overall Comparison

4.2.1 Scatter Plots

We now examine the overall performance of the re-trackers by considering all data obtained within 50km of offshore buoys (the same co-location criteria as used in [RD.4]). Figure 4 to Figure 6 display the comparison of retrieved parameters between CNES-CPP and Starlab re-trackers, by means of density plots. The colour bar indicates the number of retrievals corresponding to each box. On top of each plot, the value of the correlation is shown: the value is over 99% for all parameters.

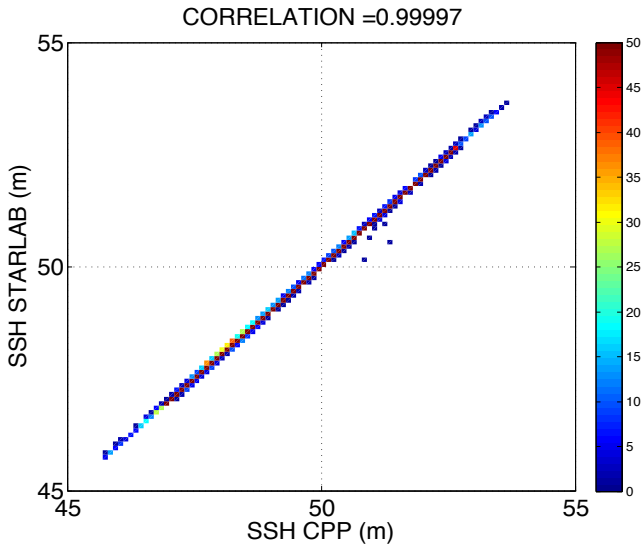

Figure 4: Scatter plot of uncorrected SSH for CNES-CPP (x-axis) versus Starlab (y-axis) for all buoys.

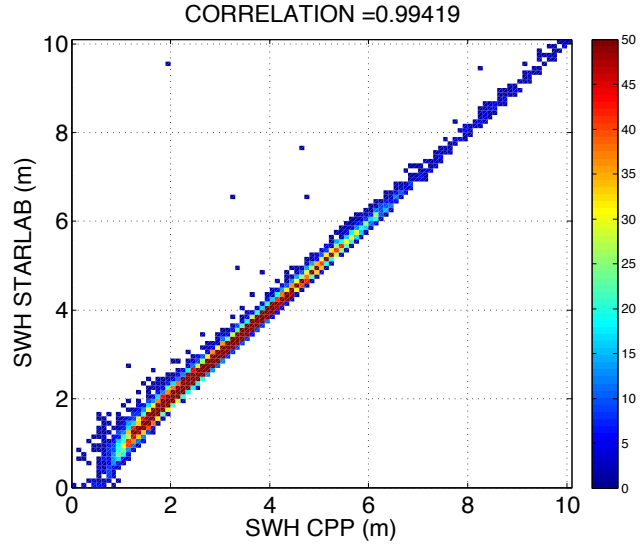

Figure 5: Scatter plot of SWH for CNES-CPP (x-axis) versus Starlab (y-axis) for all buoys.

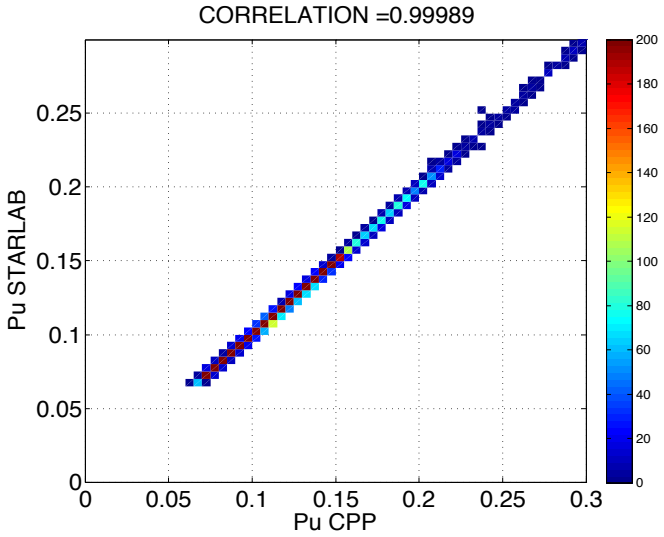

Figure 6: Scatter plot of Pu for CNES-CPP (x-axis) versus Starlab (y-axis) for all buoys.

In Figure 4 we can see that the Starlab and CNES-CPP SSH values correspond very closely across the whole range, with just a few outliers. Correlation is exact (=1) to within 5 significant figures. Similarly the agreement is very close for received power (Pu), Figure 6.

However, the correlation is less exact for SWH (Figure 5), agreement between the two data sets is good at high SWH, but there is significant scatter at low SWH, especially below 1m. It cannot be judged from this figure which data set is providing the better estimate of SWH.

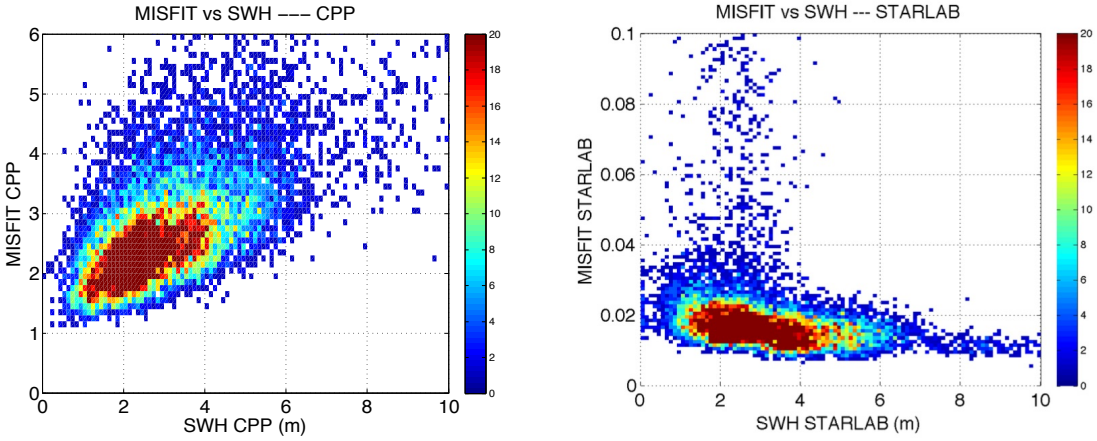

Figure 7: Misfit against SWH for CNES-CPP results (left) and Starlab (right)

Figure 7 shows the distribution of the misfit against SWH for CNES-CPP and STARLAB results by means of density plots. The misfit of CNES-CPP waveforms increases with the retrieved SWH, which is expected, given the increase of noise in measured waveforms for higher sea states [RD.4]. The opposite trend is noticed in the STARLAB dataset, together with relatively high misfit values for a group of points with 0 and 4 m of SWH. Note also the difference in the misfit scales on the y-axis.

4.2.2 Trends Against SWH

Figure 8 to Figure 10 present the trends against SWH of the difference between the two re-trackers for SSH, SWH and Pu. This is a useful way to detect differences between the re-trackers in different SWH ranges. The slope of the trends is shown on top of each plot together with the mean bias and the std of the differences. For all the parameters and in particular for SWH and Pu, the differences are particularly noticeable at low SWH. A decreasing trend is found, which might be particularly relevant for SSH estimation (-3 mm/m). The trends for SSH are more significant than the ones estimated for the difference between CNES-CPP and ESRIN R6 in RD4, but similar to those found for ESRIN R1 (see Summary and Conclusions). Given the large std compared to the slope, it is unclear whether the slopes can be considered significant. It is important to notice that the trend in SWH difference is much less than the one reported in RD4 for ESRIN R6.

In terms of mean difference between the two datasets, Starlab SSH estimations are on average 3 mm higher than the ones from CNES-CPP, which was also the case for ESRIN R6, while Starlab SWH estimations agree within 1.5 cm with the ones from CNES-CPP, a reduction compared to that reported for ESRIN R6 in RD4.

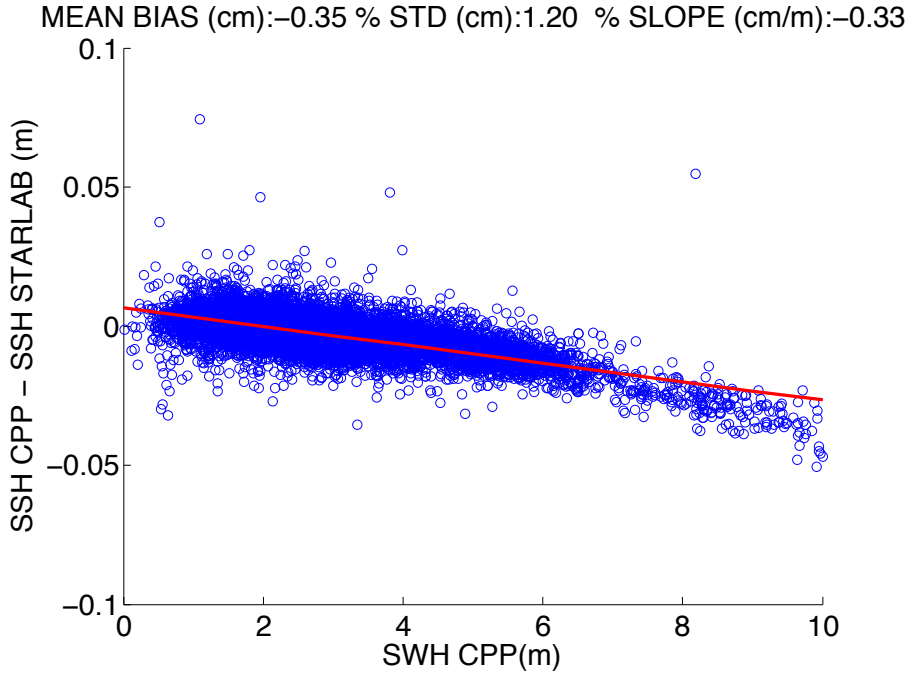

Figure 8: Behaviour and trend against CNES-CPP SWH of the CNES-CPP minus STARLAB differences in uncorrected SSH.

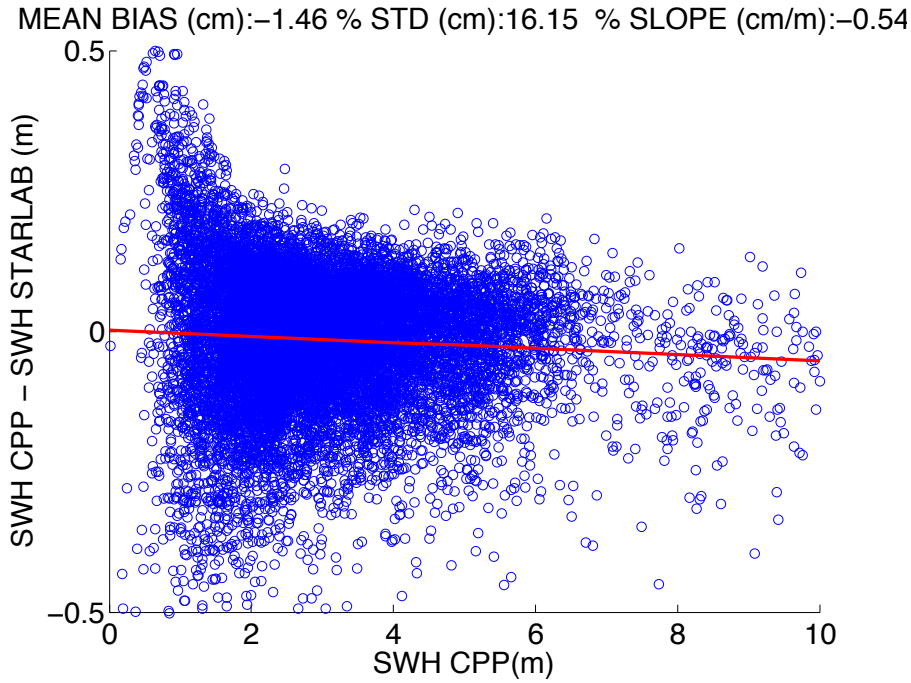

Figure 9: Behaviour and trend against CNES-CPP SWH of the CNES-CPP minus Starlab differences in SWH.

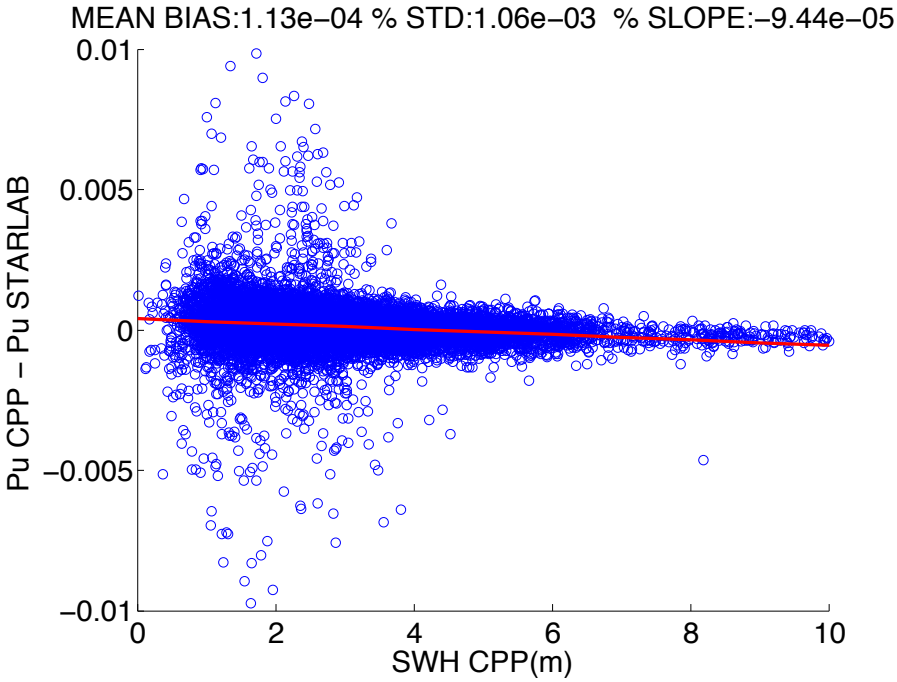

Figure 10: Behaviour and trend against CNES-CPP SWH of the CNES-CPP minus Starlab differences in Pu.

5 NOISE AS A FUNCTION OF SWH

5.1 Methodology

The method for calculating the noise (or variability) is that used in [RD.4]. Noise is estimated for SSH and SWH at 20Hz and presented as plots of noise versus SWH. The noise is estimated as the standard deviation of all valid 20Hz measurements within 1 second, averaged over 6 seconds. This provides an estimate of the mean and the variability of the noise over approximately 50km. The noise at 1Hz is estimated by scaling by sqrt (20). The mean value of the 1Hz noise is reported at the standard value of SWH = 2 meters, corresponding to the average 1Hz noise observed for all datasets with SWH between 1.5m and 2.5m.

5.2 Results

Figure 11 presents the 20Hz noise in SWH (left) and SSH (right), as a function of buoy SWH at the time of the satellite pass. In each case, the plot also shows the noise estimates from the Jason-2 LRM data obtained for the same set of buoys over the same months. The figure only includes the statistics obtained using the outer buoys (64045, 62105 and 62081) for validation, because very different results are found in terms on SSH noise depending on the location of the buoys.

A high SSH noise is found at the location of the most internal buoys (62029, 62163 and 62001), despite very good performances in terms of SWH noise, as seen in Figure 12. This figure only uses data from buoy 62029, as explained in Section 6, but similar results are found for CNES-CPP in buoys 62001 and 62163.

Higher noise might be related to the presence of significant variability across the European continental slope, in terms of tides, geophysical corrections and mean sea surface: this could explain why Jason 2 statistics are not affected by the different set of buoys, given that the RADS product of Jason 2 SSH includes the corrections. Nevertheless, this needs to be further verified and, in this validation exercise, only the outer buoys (64045, 62105 and 62081) will be considered valid for noise statistics.

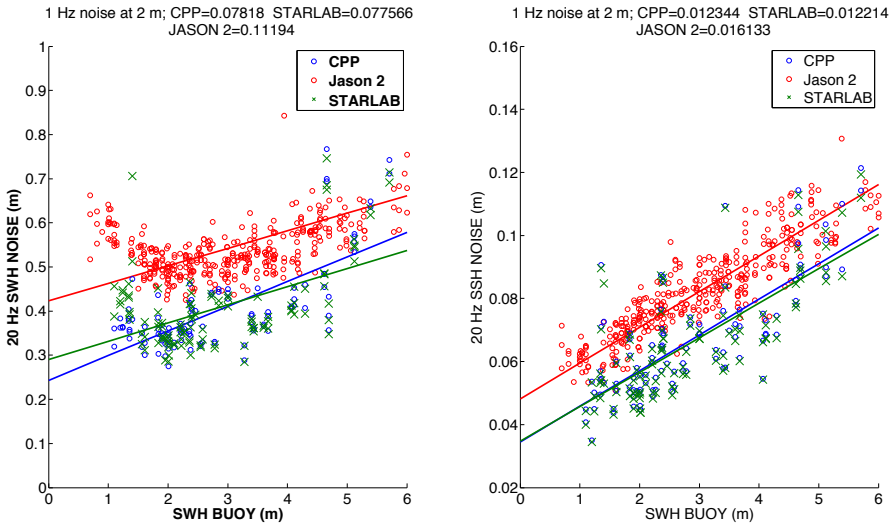

Figure 11: SSH 20Hz Noise against buoy SWH for CNES-CPP, Starlab and Jason-2 LRM at the same buoys over the same period, for "outer" buoys 64045, 62105 and 62081.

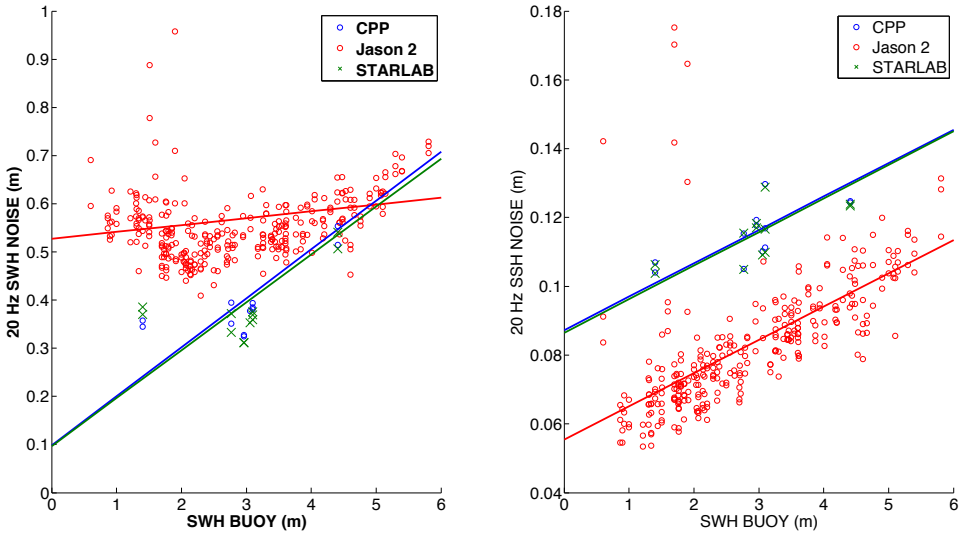

Figure 12: SWH 20Hz Noise against buoy SWH for CNES-CPP, Starlab and Jason-2 LRM at the same buoys over the same period, for buoys 62029, 62163 and 62001.

In Figure 11 it can be seen that both the C2 SAR datasets (Starlab and CNES-CPP) are significantly less noisy than Jason-2, for both SSH and SWH, confirming again that SAR altimetry can retrieve more precise values for SSH and SWH than LRM altimetry. It is less easy to see from the plots themselves any differences between the Starlab and CNES-CPP data, but we can refer to the calculated noise values, given at the top of the plots, and to the fitted lines for trends in noise against buoy SWH. From these we can see that Starlab is constantly slightly less noisy than CNES-CPP for SSH, but that for SWH Starlab is noisier for low SWH (< 1.5 m), and less noisy (than CNES-CPP) for higher SWH.

Considering the figure of noise at 2 m as reported in RD4, Starlab improves the statistics of ESRIN R1 in terms of noise on SWH and of ESRIN R6 in both SWH and SSH noise. More detail is given in Table 1 and is discussed in Section 7.

6 SATELLITE VS BUOY SWH

We present in Figure 13 the results obtained by collating C2 SAR within 50km of all buoys. The results in terms of bias and std are reported in Table 1. Overall, CNES-CPP and Starlab have very similar performances and overestimate the SWH on average by respectively 12 and 13.5 cm (the bias in table is computed as Buoy - Altimetry). The average bias is slightly more than for Jason 2, but the standard deviation is ~15 cm less.

The difference in values of CNES-CPP and Jason 2 in RD4 is probably due to the different data selection (in RD4, "...additional outlier removal is applied to remove data where SSH or SWH display excessive variability, such as in the presence of oceanic or atmospheric features (unfortunately rather frequent in these data).").

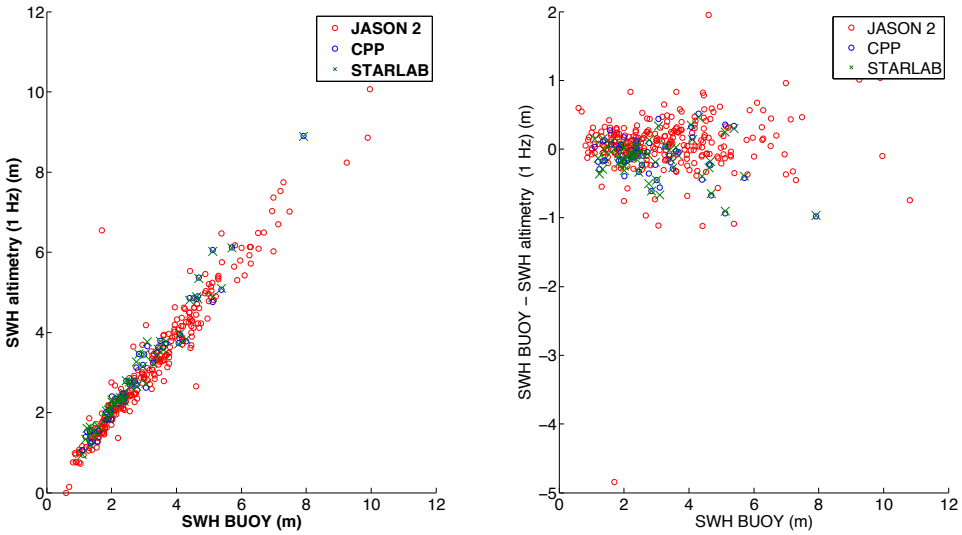

Figure 13: SWH from CNES-CPP, STARLAB and Jason 2 against buoy SWH for all buoys (left) and same plot considering the difference between satellite altimetry and the ground truth (right).

7 SUMMARY AND CONCLUSIONS

The results of the analysis are summarised in Table 1, we have included results from the RD4 to allow comparison against the full implementation of the SAMOSA model without any approximations: “ESRIN R1”, and against the implementation of the SAMOSA model in current Sentinel-3 DPM: “ESRIN R6”. However, it should be noted that the results in [RD.4] were gained from a validation data set with different coverage from that considered in this report. The data in [RD.4] covered only the 2 months July 2012 and January 2013, as opposed to the 14 months used for this study (November 2011 – December 2012) but it did include measurements from the buoys 62001 and 62163, which as discussed in the previous section, were excluded from the analysis presented here.

Run	1 Hz noise at 2m		SWH v buoy		CNES-CPP – SAMOSA difference			CNES-CPP – SAMOSA trend / m v SWH		
	SSH (cm)	**SWH (cm)**	**Bias (cm)**	**Std (cm)**	**SSH (cm)**	**SWH (cm)**	**Pu**	**SSH (cm)**	**SWH (cm)**	**Pu**
CNES-CPP	1.23	7.82	-12.0	30.0	-	-	-	-	-	-
Starlab (this study)	1.22	7.76	-13.5	28.7	-0.35	-1.46	0.00	-0.33	-0.54	0.00
ESRIN R1	1.22	8.62	5.1	22.5	0.0	1.2	3.42	-0.28	0.39	-0.013
ESRIN R6	1.25	9.25	-10.9	25.4	-0.3	17.4	-13.9	0.11	-4.76	0.002
Jason 2	1.61	11.19	6.7	45.1	-	-	-	-	-	-

Table 1: Summary diagnostics for C2 SAR CNES-CPP and STARLAB results. The values for ESRIN R1 and R6 are taken from RD4.

The main findings from these analyses are:

- There is a correlation of over 99% for all the retrieved parameters between CNES-CPP and Starlab
- The standard deviation of the bias between CNES-CPP and STARLAB is higher for low sea states.
- Both Starlab and CNES-CPP improve significantly the SSH and SWH noise performances compared to LRM altimetry.
- Starlab has slightly better noise performances than CNES-CPP. This does not hold for SWH noise when the SWH is lower than ~1.5 m, in which case Starlab is noisier than CNES-CPP.
- In terms of performance of the new implementation of the SAMOSA model with respect to previous implementations:
    - SSH Noise performance of the new model is equivalent to R1 (full SAMOSA implementation), and an improvement on R6 (current S3 DPM).
    - From the comparison against buoy SWH, the new implementation shows a larger bias and standard deviation than both R1 and R6.
    - In comparison against CNES-CPP, the new implementation of SAMOSA shows a similar bias in SSH as R6 (-3mm), whereas R1 showed no bias. For SWH the new implementation shows a bias of -1.5 cm, compared to +1.2 cm for R1 and -13.6 cm for R6.
    - The trend of SSH differences against CNES-CCP with SWH is similar for the new SAMOSA implementation and for R1 (-3mm/m), but larger than for R6

(+1mm). For SWH the trends is – 5mm /m for the new implementation, +4mm/m for R1 and -5cm / mm for R6. The Pu trends are small.

Thus we can conclude that the new implementation of SAMOSA provides a data set with a largely equivalent performance to CNES-CPP product, in terms of direct comparisons, noise performances, and validation against buoys, except at low significant wave heights, where there remain significant discrepancies between the data sets. Bearing in mind the issue of different data coverage we can also conclude that the new implementation of SAMOSA is seen to provide an improvement to the current S3 DPM, and a largely equivalent performance to the full implementation of the SAMOSA model, except in the case of a larger bias seen against buoy SWH.

The activities raised the following issues for further investigation:

- A common way of computing the misfit between the different datasets should be applied, to allow a true comparison of the impact of misfit on the two data sets, to support the development of a methodology to identify waveforms that are not well modelled, and so to build a better understanding of the causes.
- Related to the above point is the fact that a large proportion of the altimeter echoes in the CNES-CPP L1B data could not be re-tracked by the SAMOSA model. It is important that a re-tracker intended for operational implementation must be able to re-track the vast majority of uncontaminated open ocean SAR echoes. Thus it is a priority to develop a robust re-tracker that will operate reliably on uncontaminated open-ocean SAR echo data.
- A further investigation into the performance of the SAMOSA re-tracker at low wave heights is needed. The evidence of this work suggests that there is still a problem in accurately modelling SAR echoes at low wave heights.
- The high SSH noise in both the SAR datasets for buoys that are still far from the coast underlines the need of including geophysical corrections and mean sea surface to derive SSH statistics and of understanding the reason of such a high variability within 7 km of along-track data.